

Yvon Maday · Julien Salomon · Gabriel Turinici

# Monotonic time-discretized schemes in quantum control

Received: 27 October 2004 / Revised: 30 September 2005 / Published online: 21 March 2006  
© Springer-Verlag 2006

**Abstract** Most of the numerical simulations in quantum (bilinear) control have used monotonically convergent algorithms of Krotov (introduced by Tannor et al. [15]), of Zhu & Rabitz [16] or their unified formulation in [17]. However, the properties of the discrete version of these procedures have not been yet tackled with. We present in this paper a stable time and space discretization which preserves the monotonic properties of the monotonic algorithms. Numerical results show that the newly derived algorithms are stable and enable various experimentations.

## 1 Introduction

The control of quantum phenomena is a topic that has been (and is still) a source of many interesting challenges not only to physics and chemistry but also to the mathematics and applied mathematics communities [1, 2]. It is in fact the introduction of rigorous tools from the engineering literature [3],[6] that has contributed to the first successful laboratory demonstration of control over molecular phenomena [7–12].

The control interaction is modelled through a coupling operator which results in a bilinear control of the Schrödinger equation. One of the most difficult tasks remains

---

Y. Maday (✉) · J. Salomon  
Université Pierre et Marie Curie, Paris 6, Laboratoire Jacques-Louis Lions 175, rue du Chevaleret  
75013 Paris, France  
Tel.: (+33) 1 44 27 27 21  
Fax: (+33) 1 44 27 72 00  
E-mail: maday@ann.jussieu.fr, salomon@ann.jussieu.fr

G. Turinici  
INRIA Rocquencourt, Domaine de Voluceau, Rocquencourt B.P. 105,  
78153 Le Chesnay Cedex, France  
and CERMICS-ENPC, Champs sur Marne, 77455 Marne la Vallée Cedex, France  
Tel.: (+33) 1 39 63 59 68  
Fax: (+33) 1 39 63 58 82  
E-mail: gabriel.turinici@dauphine.fr

the efficient numerical simulation for the design of realistic controls. Results presented in this paper may thus be applied to other bilinear control problems, we refer the reader to [5] for a survey on this type of problems. Initially introduced by chemists and physicists, the algorithms employed to find the controls can still be improved through the introduction of more rigorous analysis ; one such analysis is presented in this paper. Here we consider the effect of time discretization on the properties of the numerical algorithms presented in the literature ; it will be seen that some important properties generally do not hold true after discretization. To cure this drawback, a class of new efficient algorithms are proposed that maintain all the required properties after discretization.

Consider a quantum system prepared in an initial state  $\psi_0$  and whose dynamics is characterized by its internal Hamiltonian  $H = H_0 + V$ . The operator  $H_0$  is the kinetic part :

$$H_0 = -\frac{1}{2} \sum_{n=1}^p \frac{1}{m_n} \Delta_{r_n},$$

where  $p$  is the number of particles considered,  $m_n$  their masses and  $\Delta_{r_n}$  the Laplacian with respect to their coordinates. The operator  $V(x)$  is the potential part. By assumption this Hamiltonian may not give rise to an appropriate evolution and an external interaction is introduced optimally to obtain the desired final property. This interaction is taken here as an electric field with time-dependent amplitude  $\varepsilon(t)$  that influences the system through a time-independent dipole moment operator  $\mu$ . The new Hamiltonian  $H - \mu\varepsilon(t)$  gives rise to the equations (we work in atomic units i.e.  $\hbar = 1$ ):

$$\begin{aligned} i \frac{\partial}{\partial t} \psi(x, t) &= H(x)\psi(x, t) - \mu(x)\varepsilon(t)\psi(x, t) \\ \psi(x, t = 0) &= \psi_0(x), \end{aligned} \tag{1}$$

where we denote by  $x$  the relevant spatial coordinates and by  $\psi_0$  the initial condition for  $\psi$  subject to the constraint  $\|\psi_0\|_2 = 1$ , where  $\|\cdot\|_2$  denotes the  $L^2$  space norm. By property of (1), the norm of the state is constant with respect to the time. In the numerical simulations, the ground state i.e. an unitary eigen vector of  $H$  associated to lowest eigen value is generally taken as initial state. Note that this equation hold on  $\mathbf{R}^N$  but for numerical tests we will consider that  $x$  belongs to an interval  $[0, L]$  and that  $\psi(t, 0) = \psi(t, L) = 0$ , for a large enough real number  $L$  and for all  $t$ . This approach is justified by physical reasons since wave functions are generally localized in a space interval.

The optimal control framework is then used to find a suitable evolution of  $\varepsilon(t)$ . The goal that the final state  $\psi(T)$  has prescribed properties is expressed by the introduction of a cost functional  $J$  to be maximized. This cost functional also includes a contribution that penalizes undesirable effects. One simple example of such a cost functional is:

$$J(\varepsilon) = \langle \psi(T) | O | \psi(T) \rangle - \alpha \int_0^T \varepsilon^2(t) dt, \tag{2}$$

where  $\alpha > 0$  is a parameter (it may also depend on time cf. [14]) and  $O$  is an observable operator that encodes the goal: the larger the value  $\langle \psi(T) | O | \psi(T) \rangle$  is,

the better the control objectives are met (here and in what follows we use the convention that for any functions  $f(x)$  and  $g(x)$  and any operator  $A$ :  $\langle f(x)|A|g(x)\rangle = \int \overline{f(x)}Ag(x)dx$ ). Note that, in general, achieving the maximal possible value of  $\langle \psi(T)|O|\psi(T)\rangle$  is at the price of a large laser fluence  $\int_0^T \varepsilon^2(t)dt$ ; the optimum evolution will therefore strike a balance between using a low laser fluence while simultaneously maximizing the desired observable.

At the maximum of the cost functional  $J(\varepsilon)$ , the Euler-Lagrange critical point equations are satisfied; a standard way to write these equations is to use a Lagrange multiplier  $\chi(x, t)$  called *adjoint state*. The following critical point equations are thus obtained [16]:

$$\begin{cases} i \frac{\partial}{\partial t} \psi(x, t) = (H(x) - \varepsilon(t)\mu(x))\psi(x, t) \\ \psi(x, t = 0) = \psi_0(x) \end{cases} \quad (3)$$

$$\begin{cases} i \frac{\partial}{\partial t} \chi(x, t) = (H(x) - \varepsilon(t)\mu(x))\chi(x, t) \\ \chi(x, t = T) = O\psi(x, T) \\ \alpha \varepsilon(t) = -Im\langle \chi | \mu | \psi \rangle(t). \end{cases} \quad (4)$$

Efficient strategies for solving in practice the critical point equations (3)-(4) are given by the monotonically convergent algorithms ([15, 16]) that are guaranteed to improve the cost functional  $J$  at each iteration. In the formulation proposed in [17], the monotonic algorithms are described by the resolution of the following equations at step  $k$ :

$$\begin{cases} i \frac{\partial}{\partial t} \psi^k(x, t) = (H(x) - \varepsilon^k(t)\mu(x))\psi^k(x, t) \\ \psi^k(x, t = 0) = \psi_0(x) \end{cases} \quad (5)$$

$$\varepsilon^k(t) = (1 - \delta)\tilde{\varepsilon}^{k-1}(t) - \frac{\delta}{\alpha} Im\langle \chi^{k-1} | \mu | \psi^k \rangle(t) \quad (6)$$

$$\begin{cases} i \frac{\partial}{\partial t} \chi^k(x, t) = (H(x) - \tilde{\varepsilon}^k(t)\mu(x))\chi^k(x, t) \\ \chi^k(x, t = T) = O\psi^k(x, T) \end{cases} \quad (7)$$

$$\tilde{\varepsilon}^k(t) = (1 - \eta)\varepsilon^k(t) - \frac{\eta}{\alpha} Im\langle \chi^k | \mu | \psi^k \rangle(t) \quad (8)$$

where  $\delta$  and  $\eta$  are 2 real parameters.

The most important property of this algorithm is given in the following theorem [17]:

**Theorem 1** *Suppose  $O$  is a self-adjoint positive semi-definite operator. Then, for any  $\eta, \delta \in [0, 2]$  the algorithm given in Eqns. (5)–(8) converges monotonically in the sense that  $J(\varepsilon^{k+1}) \geq J(\varepsilon^k)$ .*

The implementation of these algorithms involves a time-discretization which may spoil the monotonic character. Indeed a naive implementation, as the one presented straightforward [16](see also equation (25)), leads to numerical instabilities after few iterations. We study here a direct approach to discretize these algorithms so that they remain monotonic. A preliminary calculation is presented in section 2 which allows to elaborate implicit (section 3) and explicit schemes (section 4).

## 2 Preliminary

Let us choose two parameters of time discretization  $N$  and  $\Delta T$  such that  $N \Delta T = T$  and let us introduce  $\varepsilon_j, \tilde{\varepsilon}_j, \psi_j, \chi_j$  that stand respectively for approximations of  $\varepsilon(j \Delta T), \tilde{\varepsilon}(j \Delta T), \psi(j \Delta T), \chi(j \Delta T)$ . We denote in the following  $\underline{\varepsilon} = (\varepsilon_j)_{0 \leq j \leq N}$ ,  $\tilde{\underline{\varepsilon}} = (\tilde{\varepsilon}_j)_{0 \leq j \leq N}$ ,  $\underline{\psi} = (\psi_j)_{0 \leq j \leq N}$ ,  $\underline{\chi} = (\chi_j)_{0 \leq j \leq N}$ .

A simple approach would adopt the first-order split-operator method but for higher accuracy, we prefer a propagation method based on the second-order split-operator technique. This method also simplifies algebraic manipulations as it will appear later (see equation (12)).

In this part, for any prescribed sets  $\underline{\varepsilon}, \tilde{\underline{\varepsilon}}$ , the computation of the state  $\underline{\psi}$  and the adjoint state  $\underline{\chi}$  is thus defined through a Strang-second-order split-operator method [13] (see also [16, 18, 20]) leading to the semi-discretized propagation equations:

$$\begin{cases} \psi_{j+1} = e^{\frac{H_0 \Delta T}{2i}} e^{\frac{V - \mu \varepsilon_j}{i} \Delta T} e^{\frac{H_0 \Delta T}{2i}} \psi_j \\ \psi_0 = \psi_{init}, \end{cases} \quad (9)$$

$$\begin{cases} \chi_{j-1} = e^{-\frac{H_0 \Delta T}{2i}} e^{\frac{-V + \mu \tilde{\varepsilon}_{j-1}}{i} \Delta T} e^{-\frac{H_0 \Delta T}{2i}} \chi_j \\ \chi_N = O \psi_N. \end{cases} \quad (10)$$

The full (time-space) discretization of these equations is described in the section 5. In what follows, the initial value  $\psi_{init}$  will be simply denoted  $\psi_0$ . We suppose that  $\|\psi_0\|_2 = 1$ . Note that this discretization of (3) and (4) preserves the norm of the propagated vectors in the sense that:

$$\forall j, 0 \leq j \leq N-1, \quad \|\psi_{j+1}^k\|_2 = 1, \quad \|\chi_j^{k-1}\|_2 = \|\chi_N^{k-1}\|_2 = \|O \psi_N^{k-1}\|_2. \quad (11)$$

Let us consider the time discretization of the cost functional (2):

$$J_{\Delta T}(\varepsilon) = \langle \psi_N | O | \psi_N \rangle - \alpha \Delta T \sum_{j=0}^{N-1} \varepsilon_j^2.$$

Assuming that another set of control amplitudes  $\underline{\varepsilon}'$  is given, with associated state  $\underline{\psi}'$  and adjoint state  $\underline{\chi}'$ , we analyse the difference in the cost functional:

$$\begin{aligned} J_{\Delta T}(\underline{\varepsilon}') - J_{\Delta T}(\underline{\varepsilon}) &= \langle \psi'_N - \psi_N | O | \psi'_N - \psi_N \rangle \\ &\quad + 2Re \langle \psi'_N - \psi_N | O | \psi_N \rangle + \alpha \Delta T \left( \sum_{j=0}^{N-1} \varepsilon_j'^2 - \varepsilon_j^2 \right). \end{aligned}$$

Focusing on  $\langle \psi'_N - \psi_N | O | \psi_N \rangle$ , we find:

$$\begin{aligned}
 \langle \psi'_N - \psi_N | O | \psi_N \rangle &= \langle \psi'_N - \psi_N, \chi_N \rangle \\
 &= \sum_{j=0}^{N-1} \langle \psi'_{j+1} - \psi_{j+1}, \chi_{j+1} - \chi_j \rangle \\
 &\quad + \langle \psi'_{j+1} - \psi_{j+1} - \psi'_j + \psi_j, \chi_j \rangle \\
 &= \sum_{j=0}^{N-1} \langle \psi'_{j+1} - \psi_{j+1}, (e^{\frac{H_0 \Delta T}{2i}} e^{\frac{V - \mu \tilde{\varepsilon}_j}{i} \Delta T} e^{\frac{H_0 \Delta T}{2i}} - 1) \chi_j \rangle \\
 &\quad + \sum_{j=0}^{N-1} \langle (1 - e^{-\frac{H_0 \Delta T}{2i}} e^{\frac{-V + \mu \varepsilon'_j}{i} \Delta T} e^{-\frac{H_0 \Delta T}{2i}}) \psi'_{j+1}, \chi_j \rangle \\
 &\quad - \sum_{j=0}^{N-1} \langle (1 - e^{-\frac{H_0 \Delta T}{2i}} e^{\frac{-V + \mu \varepsilon_j}{i} \Delta T} e^{-\frac{H_0 \Delta T}{2i}}) \psi_{j+1}, \chi_j \rangle. \quad (12)
 \end{aligned}$$

Let us introduce now  $\tilde{\psi}_j = e^{-\frac{H_0 \Delta T}{2i}} \psi_j$ ,  $\check{\psi}_j = e^{\frac{H_0 \Delta T}{2i}} \psi_j$ ,  $\check{\chi}_j = e^{-\frac{H_0 \Delta T}{2i}} \chi_j$ ,  $\tilde{\chi}_j = e^{\frac{H_0 \Delta T}{2i}} \chi_j$  so that:

$$\begin{aligned}
 \langle \psi'_N - \psi_N | O | \psi_N \rangle &= \sum_{j=0}^{N-1} \langle (e^{\frac{\mu(\tilde{\varepsilon}_j - \varepsilon'_j)}{i} \Delta T} - 1) \check{\psi}'_j, \tilde{\chi}_j \rangle \\
 &\quad + \langle \tilde{\psi}_{j+1}, (e^{\frac{\mu(\tilde{\varepsilon}_j - \varepsilon_j)}{i} \Delta T} - 1) \check{\chi}_{j+1} \rangle.
 \end{aligned}$$

Thus, defining an approximation of  $\mu$  by:

$$\mu^* : (x, y) \mapsto i \frac{e^{\frac{\mu(x-y)}{i} \Delta T} - 1}{\Delta T(x-y)}, \quad (13)$$

and

$$\begin{cases} a_j(x, y) = -\frac{1}{\alpha} \text{Im} \langle \tilde{\chi}_j | \mu^*(x, y) | \check{\psi}'_j \rangle \\ b_j(x, y) = -\frac{1}{\alpha} \text{Im} \langle \check{\chi}_j | \mu^*(x, y) | \check{\psi}_j \rangle, \end{cases} \quad (14)$$

we have:

$$\begin{aligned}
 \text{Re} \langle \psi'_N - \psi_N | O | \psi_N \rangle &= \alpha \Delta T \sum_{j=0}^{N-1} a_j(\tilde{\varepsilon}_j, \varepsilon'_j) (\varepsilon'_j - \tilde{\varepsilon}_j) \\
 &\quad + b_{j+1}(\varepsilon_j, \tilde{\varepsilon}_j) (\tilde{\varepsilon}_j - \varepsilon_j).
 \end{aligned}$$

Finally we obtain the formula:

$$\begin{aligned}
J_{\Delta T}(\underline{\varepsilon}') - J_{\Delta T}(\underline{\varepsilon}) &= \langle \psi'_N - \psi_N | \mathcal{O} | \psi'_N - \psi_N \rangle \\
&+ \alpha \Delta T \sum_{j=0}^{N-1} \left[ \underbrace{(\tilde{\varepsilon}_j - a_j(\tilde{\varepsilon}_j, \varepsilon'_j))^2 - (\varepsilon'_j - a_j(\tilde{\varepsilon}_j, \varepsilon'_j))^2}_{\phi_j(\tilde{\varepsilon}_j, \varepsilon'_j)} \right. \\
&\left. + \underbrace{(\varepsilon_j - b_{j+1}(\varepsilon_j, \tilde{\varepsilon}_j))^2 - (\tilde{\varepsilon}_j - b_{j+1}(\varepsilon_j, \tilde{\varepsilon}_j))^2}_{\tilde{\phi}_j(\varepsilon_j, \tilde{\varepsilon}_j)} \right], \quad (15)
\end{aligned}$$

This formula will help us designing schemes that remain monotonic after the discretization in time. Indeed a negative part of each sum's components appears explicitly. Canceling out or minimizing these terms will enable us to design monotonic schemes: given a field  $\underline{\varepsilon}^k$ , the analysis of the negative part of  $\tilde{\phi}_j(\varepsilon_j^k, \tilde{\varepsilon}_j^k)$  for each  $j$  defines the sequence  $\tilde{\varepsilon}^k$  and the analysis of the negative part of  $\phi_j(\tilde{\varepsilon}_j^k, \varepsilon_j^{k+1})$  defines  $\varepsilon^{k+1}$ .

*Remark 1* In fact  $a_j(x, y)$ ,  $b_j(x, y)$ ,  $\phi_j(\tilde{\varepsilon}_j, \varepsilon'_j)$  and  $\tilde{\phi}_j(\varepsilon_j, \tilde{\varepsilon}_j)$  also depend on  $\underline{\varepsilon}$ ,  $\underline{\varepsilon}'$  and  $\tilde{\varepsilon}$  which are used to propagate states and adjoint states. In order to simplify notations, we have omitted these dependencies throughout this paper.

### 3 Implicit scheme

A first simple idea consists in canceling out the negative parts of  $\phi_j$  and  $\tilde{\phi}_j$ . This leads us to define implicitly the control amplitudes. The following procedure is thus obtained.

#### 3.1 Algorithm

Given initial control amplitudes  $\underline{\varepsilon}^0, \tilde{\varepsilon}^0$  and their associated state  $\psi^0$  and adjoint state  $\chi^0$ , suppose that  $\underline{\psi}^k, \underline{\chi}^k, \underline{\varepsilon}^k, \tilde{\varepsilon}^k$  have already been computed. Let us define just as in (14) (see remark 1):

$$\begin{cases} a_j^k(x, y) = -\frac{1}{\alpha} \text{Im} \langle \tilde{\chi}_j^k | \mu^*(x, y) | \check{\psi}_j^{k+1} \rangle \\ b_j^k(x, y) = -\frac{1}{\alpha} \text{Im} \langle \check{\chi}_j^k | \mu^*(x, y) | \tilde{\psi}_j^k \rangle, \end{cases}$$

The derivation of  $\underline{\psi}^{k+1}, \underline{\chi}^{k+1}, \underline{\varepsilon}^{k+1}, \tilde{\varepsilon}^{k+1}$  is done as follows:

Step 1: Knowing  $\underline{\psi}_0^{k+1}$ , define  $\underline{\psi}_{j+1}^{k+1}$  recursively from  $\underline{\psi}_j^{k+1}$  by:

- Compute  $\varepsilon_j^{k+1}$  by:

$$\varepsilon_j^{k+1} = a_j^k(\tilde{\varepsilon}_j^k, \varepsilon_j^{k+1}). \quad (16)$$

- Compute  $\underline{\psi}_{j+1}^{k+1}$  from (9).

Step 2: Knowing  $\chi_N^{k+1}$ , define  $\chi_j^{k+1}$  recursively from  $\chi_{j+1}^{k+1}$  by:

- Compute  $\tilde{\varepsilon}_j^{k+1}$  by:

$$\tilde{\varepsilon}_j^{k+1} = b_{j+1}^{k+1}(\varepsilon_j^{k+1}, \tilde{\varepsilon}_j^{k+1}). \quad (17)$$

- Compute  $\chi_j^{k+1}$  from (10).

This algorithm is by construction a monotonic discretization of the monotonic scheme described in [16]. A more general procedure, corresponding to the implicit discretization of the class of monotonic schemes class introduced in [17], consists in replacing equations (16) and (17) by the following:

$$\begin{cases} \varepsilon_j^{k+1} = (1 - \delta)\tilde{\varepsilon}_j^k + \delta a_j^k(\tilde{\varepsilon}_j^k, \varepsilon_j^{k+1}) \\ \tilde{\varepsilon}_j^{k+1} = (1 - \eta)\varepsilon_j^{k+1} + \eta b_{j+1}^{k+1}(\varepsilon_j^{k+1}, \tilde{\varepsilon}_j^{k+1}). \end{cases} \quad (18)$$

**Theorem 2** *If  $(\delta, \eta) \in [0, 2]^2$ , definitions (18) preserve the monotonicity of the implicit scheme.*

*Proof* For  $\delta \neq 0$  and  $\eta \neq 0$ , using the definitions (18) of  $\varepsilon_j^{k+1}$  and  $\tilde{\varepsilon}_j^{k+1}$ , the computation which led to (15) becomes:

$$\begin{aligned} J_{\Delta T}(\varepsilon^{k+1}) - J_{\Delta T}(\varepsilon^k) &= \langle \psi_N^{k+1} - \psi_N^k | O | \psi_N^{k+1} - \psi_N^k \rangle \\ &\quad + \alpha \Delta T \sum_{j=0}^{N-1} \left( \frac{2}{\delta} - 1 \right) (\tilde{\varepsilon}_j^k - \varepsilon_j^{k+1})^2 \\ &\quad + \left( \frac{2}{\eta} - 1 \right) (\varepsilon_j^k - \tilde{\varepsilon}_j^k)^2, \end{aligned}$$

from which monotonicity follows.  $\square$

*Remark 2* The following definition for control amplitudes also lead to monotonic scheme:

$$\begin{cases} \varepsilon_j^{k+1} = (1 - \delta)\tilde{\varepsilon}_{j-1}^k - \frac{\delta}{\alpha} \operatorname{Re} \langle \tilde{\chi}_j^k | e^{\frac{\mu(\tilde{\varepsilon}_j^k - \varepsilon_j^{k+1})}{i} \Delta T} - 1 | \check{\psi}_j^{k+1} \rangle \\ \tilde{\varepsilon}_j^{k+1} = (1 - \eta)\varepsilon_{j+1}^{k+1} - \frac{\eta}{\alpha} \operatorname{Re} \langle \check{\chi}_{j+1}^{k+1} | e^{\frac{\mu(\tilde{\varepsilon}_{j+1}^{k+1} - \varepsilon_{j+1}^{k+1})}{i} \Delta T} - 1 | \tilde{\psi}_{j+1}^{k+1} \rangle. \end{cases}$$

Note that (18) can be written the same way:

$$\begin{cases} \varepsilon_j^{k+1} = (1 - \delta)\tilde{\varepsilon}_j^k - \frac{\delta}{\alpha} \operatorname{Re} \langle \tilde{\chi}_j^k | e^{\frac{\mu(\tilde{\varepsilon}_j^k - \varepsilon_j^{k+1})}{i} \Delta T} - 1 | \check{\psi}_j^{k+1} \rangle \\ \tilde{\varepsilon}_j^{k+1} = (1 - \eta)\varepsilon_j^{k+1} - \frac{\eta}{\alpha} \operatorname{Re} \langle \check{\chi}_{j+1}^{k+1} | e^{\frac{\mu(\tilde{\varepsilon}_j^{k+1} - \varepsilon_j^{k+1})}{i} \Delta T} - 1 | \tilde{\psi}_{j+1}^{k+1} \rangle. \end{cases}$$

### 3.2 Existence and uniqueness of solutions

This subsection is devoted to the analysis of (18).

**Theorem 3** *Suppose that (18) admits the solutions  $\varepsilon_j^{k+1}$  and  $\tilde{\varepsilon}_j^{k+1}$ ; then there exists  $M > 0$ , depending only on  $\delta, \eta, \alpha, \|O\|_\infty$  and  $\|\mu\|_\infty$  such that:*

$$\forall k \in N, \forall j, 0 \leq j \leq N, |\varepsilon_j^{k+1}| \leq M, |\tilde{\varepsilon}_j^{k+1}| \leq M.$$

*Proof* Let us compute an upper bound for  $a_j^k$ . First, the mean value inequality yields:

$$\forall X, Y \in \mathbf{R}, \frac{|e^{\frac{\mu(X-Y)}{i} \Delta T} - 1|}{|X - Y| \Delta T} \leq \|\mu\|_\infty, \quad (19)$$

from which we deduce that  $\|\mu^*\|_\infty \leq \|\mu\|_\infty$  from the definition (13). Secondly state and adjoint state verify (11). Then:

$$\|\psi_{j+1}^k\|_2 = 1, \quad \|\chi_j^{k-1}\|_2 = \|O\psi_N^{k-1}\|_2 \leq \|O\|_\infty \|\psi_N^{k-1}\|_2 = \|O\|_\infty.$$

Thanks to the Cauchy-Schwartz inequality, the inequality (19) and the definition (14) of  $a_j^k$  give:

$$\forall X, Y \in \mathbf{R}, |a_j^k(X, Y)| \leq \frac{\|O\|_\infty \|\mu\|_\infty}{\alpha}.$$

Let us define  $M$  by:

$$M = \max(\|\underline{\varepsilon}^0\|_\infty, \max(1, \frac{\delta}{2 - \delta}, \frac{\eta}{2 - \eta}) \frac{\|O\|_\infty \|\mu\|_\infty}{\alpha}), \quad (20)$$

and assume  $|\varepsilon_j^k| \leq M$  and  $|\tilde{\varepsilon}_j^k| \leq M$  have been obtained, then:

$$\begin{aligned} |\varepsilon_j^{k+1}| &\leq |1 - \delta|M + \delta|a_j^k(\varepsilon_j^k, \varepsilon_j^{k+1})|. \\ |\varepsilon_j^k| &\leq |1 - \delta|M + \delta \frac{\|O\|_\infty \|\mu\|_\infty}{\alpha}. \end{aligned}$$

If  $\delta \leq 1$  then  $M = \frac{\|O\|_\infty \|\mu\|_\infty}{\alpha}$  and  $|\varepsilon_j^k| \leq |1 - \delta|M + \delta M = M$ , otherwise  $M = \frac{\delta}{2 - \delta} \frac{\|O\|_\infty \|\mu\|_\infty}{\alpha}$  and in this case  $|\varepsilon_j^k| \leq |1 - \delta|M + \delta \frac{2 - \delta}{\delta} M = (\delta - 1)M + (2 - \delta)M = M$ . Which ends the proof by induction. We leave to the reader the proof concerning  $\tilde{\varepsilon}_j^{k+1}$ , which is quite similar.  $\square$

**Theorem 4** *Assume  $\|O\|_\infty, \|\mu\|_\infty$  are bounded, then there exists a solution  $(\varepsilon_j^{k+1}, \tilde{\varepsilon}_j^{k+1})$  of the system (18).*

*Proof* Given a field  $\tilde{\varepsilon}^k$ , the theorem 3 proves that  $f : x \mapsto (1 - \delta)\tilde{\varepsilon}_j^k + \delta a_j^k(\tilde{\varepsilon}_j^k, x)$  maps the interval  $[-M, M]$ , where  $M$  is defined by (20), onto itself. The intermediate value theorem states that there exists a fixed-point for  $f$  in  $[-M, M]$ . Here again, we leave to the reader the proof concerning  $\tilde{\varepsilon}_j^{k+1}$ .  $\square$

In order to solve (18), Picard's fixed-point theorem can be used. We precise in the next theorem sufficient conditions for this method to converge.

**Theorem 5** Given  $\tilde{\varepsilon}^{k+1}$ , if:

$$\frac{\delta}{\alpha} \|O\|_{\infty} \|\mu\|_{\infty}^2 \Delta T < 1, \quad (21)$$

then the sequence  $(u_n)$  defined as follows:

$$u_0 \in [-M, M], \quad u_{n+1} = f(u_n),$$

where  $f$  is defined in the proof of theorem 4, converges towards the unique solution of the system (18).

*Proof* In the following computations,  $\mu$  denotes both the spacial function and its evaluation in an unspecified point. Consider the function  $h$  defined as follows:

$$h(\theta) = \frac{e^{i\theta} - 1}{\theta}.$$

With this definition  $\mu^*$  from (13) can be expressed as:

$$\mu^*(\tilde{\varepsilon}_j^{k-1}, x) = -i\mu h(\mu(x - \tilde{\varepsilon}_j^{k-1})\Delta T).$$

Since  $\frac{d\mu^*(\tilde{\varepsilon}_j^{k-1}, x)}{dx} = -i\mu^2 \Delta T h'(\mu \Delta T (x - \tilde{\varepsilon}_j^{k-1}))$  and the fact that one can easily prove that  $|h'(\theta)| \leq 1$ , the mean value inequality gives:

$$|\mu^*(\tilde{\varepsilon}_j^{k-1}, x) - \mu^*(\tilde{\varepsilon}_j^{k-1}, y)| \leq \|\mu\|_{\infty}^2 \Delta T |x - y|.$$

From the definitions (14) and (18), we conclude:

$$|f(x) - f(y)| \leq \frac{\delta}{\alpha} \|O\|_{\infty} \|\mu\|_{\infty}^2 \Delta T |x - y|.$$

which provides the contraction condition under the assumption (21).  $\square$

### 3.3 Remarks on the Newton method

Instead of considering the equation  $f(x) = x$ , the Newton method suggests to consider the equation  $g(x) = x$ , where  $g(x) = x - \frac{f(x)-x}{f'(x)-1}$ . If  $x_0$  is the solution of the latest equation and  $x$  a real number, there exists  $c_x$  between  $x$  and  $x_0$  such that:

$$g(x) - g(x_0) = g''(c_x) \frac{(x - x_0)^2}{2}.$$

A coarse estimate of  $g''(c_x)$  can be done by using the continuity of  $g''$ . Indeed, we can approximate this quantity by  $g''(x_0)$ . A simple computation leads then to the inequality:

$$|g''(x_0)| \leq \frac{\|O\|_{\infty} \|\mu\|_{\infty}^3 \Delta T^2}{1 - \frac{\delta}{\alpha} \|O\|_{\infty} \|\mu\|_{\infty}^2 \Delta T}. \quad (22)$$

Note that the denominator in the previous fraction is not equal to zero as soon as the hypothesis of the theorem 4 is fulfilled. The estimation (22) can be used to give a hint on the speed of convergence of the Newton method.

### 3.4 Numerical results

In order to test the performance of the algorithm, a case already treated in the literature was chosen [16]. The system under consideration is the  $O - H$  bond that vibrates in a Morse type potential  $V(x)$  given by:

$$V(x) = D_0((e^{-\beta(x-x_0)} - 1)^2 - 1).$$

We refer the reader to [16] for the numerical details concerning this system. The goal is to localize the wave packet at a given location  $x'$ ; this is expressed through the requirement that  $\langle \psi(T) | O | \psi(T) \rangle$  is maximized, where the observable  $O$  is  $O(x) = \frac{\gamma_0}{\sqrt{\pi}} e^{-\gamma_0^2(x-x')^2}$ . Numerical tests carried out on this example show that although initial iterations of the algorithm are monotonic, starting with a given iteration numerical instabilities are developed as illustrated in Fig.1. In a first test parameters  $\delta$  and  $\eta$  are chosen equal to 1. To solve (18), the Newton method was used, which displays good performance for  $\Delta T \leq 50$ . In other cases bisection method was used successfully. In order to test results of [17] we have compared the case  $\delta = 1, \eta = 1$  which corresponds to [16] with the case  $\delta = 2, \eta = 0$ . Results represented in Fig.1 prove that even if this latter leads to a faster convergence during the first iterations, the level reached by the cost functional is lower than

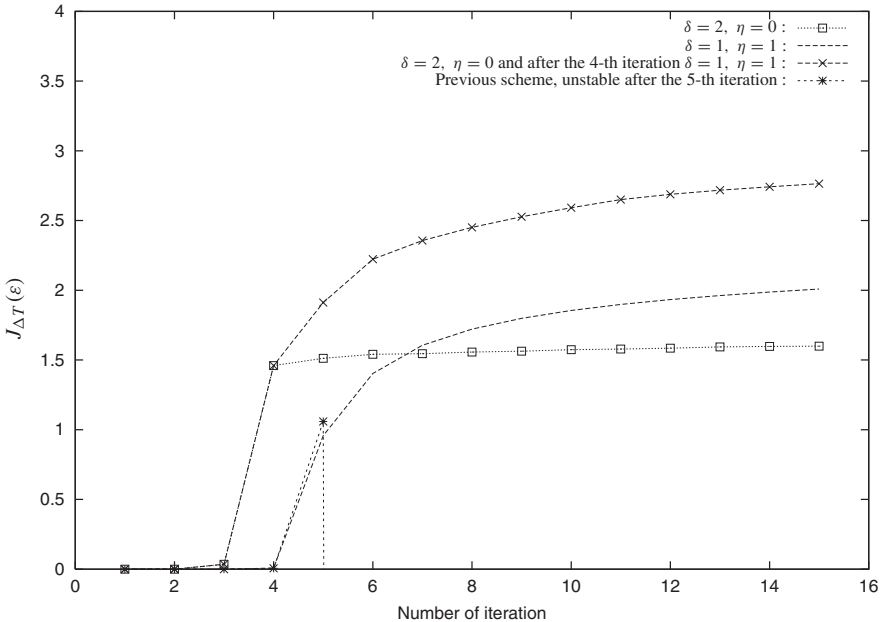


**Fig. 1** Numerical instabilities which occurred with schemes that are not monotonic after discretization has hidden the better performance of the choice  $\delta = 1, \eta = 1$  appearing after iteration  $k = 6$ . The change of the parameters  $(\delta, \eta) = (2, 0) \rightarrow (1, 1)$  at the 4-th iteration appears to be very efficient

in the first case. A good methodology may consist in starting with  $\delta = 2$ ,  $\eta = 0$ , then switch to  $\delta = 1$ ,  $\eta = 1$  (see Fig. 1).

## 4 Explicit scheme

The formula (15) allows also to define an explicit scheme, which facilitates the implementation with respect to the implicit scheme and thus decreases the overall computational complexity.

### 4.1 Algorithm

As above, we only develop the method to propagate  $\psi_j^{k+1}$  with  $\varepsilon_j^{k+1}$ . Consider the mapping  $f_j : x \mapsto (\tilde{\varepsilon}_j^k - a_j^k(\tilde{\varepsilon}_j^k, x))^2 - (x - a_j^k(\tilde{\varepsilon}_j^k, x))^2$ . The optimal choice of  $\varepsilon_j^{k+1}$  corresponds to the maximum of  $f_j$ . To localize this point one approximates  $f_j$  by its second order expansion in a neighborhood of  $x = \tilde{\varepsilon}_j^k$ . Note that this value cancels  $f_j$ . Let us define  $h = x - \tilde{\varepsilon}_j^k$  and develop the expression:

$$\begin{aligned}
 a_j^k(\tilde{\varepsilon}_j^k, \tilde{\varepsilon}_j^k + h) &= -\frac{1}{\alpha} \text{Im} \langle \tilde{\chi}_j^k | \mu^*(\tilde{\varepsilon}_j^k, \tilde{\varepsilon}_j^k + h) | \check{\psi}_j^{k+1} \rangle \\
 &= \underbrace{-\frac{1}{\alpha} \text{Im} \langle \tilde{\chi}_j^k | \mu | \check{\psi}_j^{k+1} \rangle}_{\varepsilon_0} \\
 &\quad - h \underbrace{\frac{\Delta T}{2\alpha} \text{Re} \langle \tilde{\chi}_j^k | \mu^2 | \check{\psi}_j^{k+1} \rangle}_{\varepsilon_1} \\
 &\quad + h^2 \underbrace{\frac{\Delta T^2}{6\alpha} \text{Im} \langle \tilde{\chi}_j^k | \mu^3 | \check{\psi}_j^{k+1} \rangle}_{\varepsilon_2} + o(h^2), \tag{23}
 \end{aligned}$$

that leads to:

$$\begin{aligned}
 f_j(\tilde{\varepsilon}_j^k, \tilde{\varepsilon}_j^k + h) &= (\tilde{\varepsilon}_j^k - \varepsilon_0 + \varepsilon_1 h - \varepsilon_2 h^2)^2 \\
 &\quad - (\tilde{\varepsilon}_j^k + h - \varepsilon_0 + \varepsilon_1 h - \varepsilon_2 h^2)^2 + o(h^2).
 \end{aligned}$$

The maximum of this polynomial in  $h$  is achieved for

$$h_m = \frac{\varepsilon_0 - \tilde{\varepsilon}_j^k}{2\varepsilon_1 + 1}, \tag{24}$$

which allows to define  $\varepsilon_j^{k+1} = \tilde{\varepsilon}_j^k + h_m$ . A similar formula can be obtained for  $\tilde{\varepsilon}_j^{k+1}$ . The explicit scheme consists in replacing (16) and (17) in the implicit scheme by these equations.

## 4.2 Cost of the algorithm

The complexity of this algorithm can be compared with the first order scheme described in [16]:

$$\begin{cases} \varepsilon_j^{k+1} = -\frac{1}{\alpha} \text{Im} \langle \chi_j^k | \mu | \psi_j^k \rangle \\ \tilde{\varepsilon}_j^{k+1} = -\frac{1}{\alpha} \text{Im} \langle \chi_j^k | \mu | \psi_j^{k+1} \rangle. \end{cases} \quad (25)$$

Note that this original scheme may develop numerical instabilities after a few iterations.

The only additional cost consists in the computation of  $\varepsilon_1$  (see equation (23)). The Fig.2 represents the computational cost of the explicit and standard schemes. Moreover storage space is the same since the intermediate values to store are in one case  $\chi_j$  and  $\psi_j$  and in the other  $\tilde{\chi}_j$  and  $\tilde{\psi}_j$ .

## 4.3 Numerical results

This algorithm has been tested on the previous example. Results show that, for  $\Delta T \leq 50$  the explicit scheme is more efficient than the implicit one: for  $\Delta T = 10$  and after 6 iterations,  $J$  reaches 1.687, instead of 1.406 with the implicit scheme. In addition the time of computation is divided by more than 2. The evolution of the values of the cost functional with implicit and explicit schemes is presented in Fig. 3.

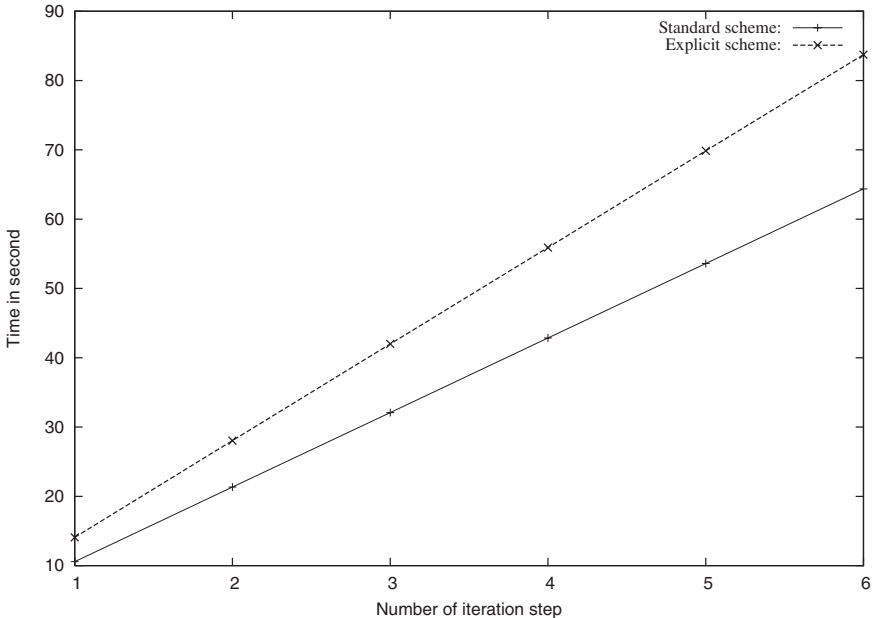


**Fig. 2** Explicit scheme requires 22% more time than the standard one (see equation (25)). The standard scheme is numerically unstable after the seventh iteration

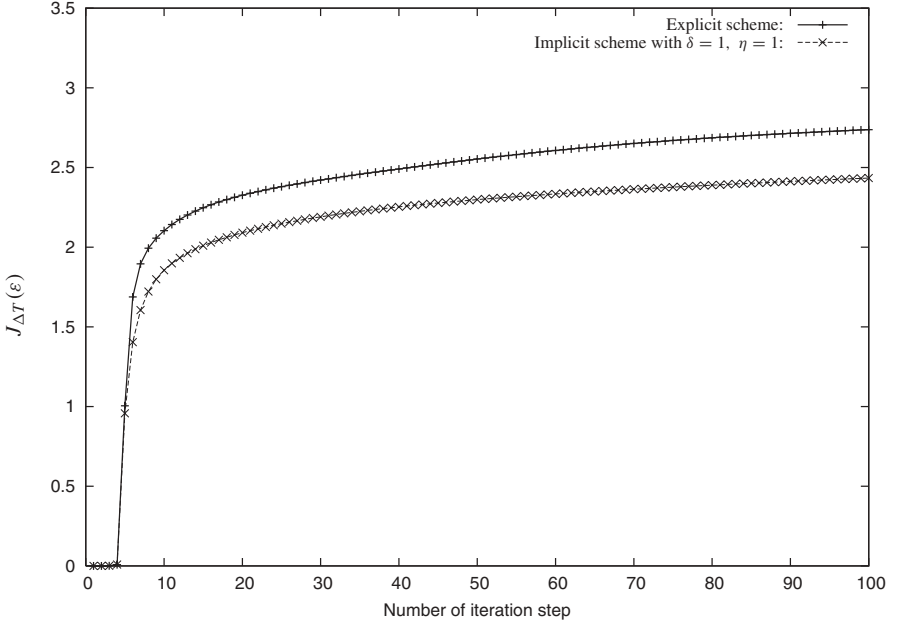


**Fig. 3** Evolution of the cost functional with implicit ( $\delta = 1$ ,  $\eta = 1$ ) and explicit schemes

We have also observed that the choice of  $h = \frac{\varepsilon_0 - \tilde{\varepsilon}_j^k}{2\varepsilon_1 + 1}$  is close to optimal choice: with this value  $\phi_j^{k+1}(\tilde{\varepsilon}_j^k, \tilde{\varepsilon}_j^k + h)$  has always been found to be positive. We have also tested different choices for  $h$  by  $h/2$ ,  $2h$  or canceling  $\varepsilon_1$ . All these tests lead to a lower value of  $J$ .

#### 4.4 Remark on a change of time step discretization

Both previous schemes provide satisfying results for a large range of discretization time steps. We can take advantage of this fact by changing the value of  $\Delta T$  during the computations. In some cases this strategy accelerates the computations and sometimes gives a better initial guess. Given  $\Delta T$  and  $\Delta t$  (a large and a small time-step), some iterations are carried out with the large time-step  $\Delta T$ . Then, the field is interpolated on the finer time grid associated with  $\Delta t$  and the algorithm is restarted with this new field as initial value.

This approach may be justified by the fact that with our current choice  $O\psi_N^0 = 0$ , leading to  $\chi_j^0 = 0$  for all  $j < N$ , consequently and the standard initial value of the field  $\varepsilon^0 = 0$  is a critical point of  $J_{\Delta T}$ . In practice, numerical errors allow the algorithm to escape from this critical point which in some sense is numerically unstable (see for example the first values of  $J_{\Delta T}$  in Fig. 1 or in Fig. 3). A large time step allows to increase these errors and accelerate the optimization process. This method has been tested on the previous example with the implicit scheme: 5 iterations with  $\Delta T = 10$  have been performed then 10 with  $\Delta t = 5$ . After these

15 iterations the cost functional  $J$  reaches 2.69 instead of 2.19 with a constant time step  $\Delta T = 5$ . Thus results are better on two points: value of  $J$  is higher and time is divided by 9. These facts are represented in Fig. 4.

## 5 Full discretization

All the calculations developed in the preliminary part have been done assuming that no spatial approximation is used. In practice, we must also choose an appropriate discretization method to represent the functions and evaluate the spacial hermitian products. The original problem is set on  $\mathbf{R}$  and, as is classical and already told in the introduction, we restrict the problem to a bounded interval and impose homogeneous Dirichlet boundary conditions to supplement the state equations. The interval is denoted as  $[0, L]$  for a large enough real number  $L$ . The set of all regular enough functions over  $[0, L]$  that vanish in 0 and  $L$  is then considered as the set of restrictions to  $]0, L[$  of the set of all odd,  $2L$ -periodic functions of  $\mathbf{R}$ . The discretization then proceeds having in mind the Fourier-spectral method. Let us introduce a discretization parameter  $M$ , the spacial approximation is based on the set of all odd,  $2L$ -periodic functions of (trigonometric) degree  $\leq M$ . We first notice that the kinetic part of the the Hamiltonian operator (Laplace operator) is diagonal in the Fourier basis. Second, we notice that, in opposition, the potential part  $V - \mu\varepsilon$  is multiplicative in the “physical” space. We thus introduce the points  $x_i = \frac{i}{M+1}L$ . The discrete state functions are sampled at these points and the unknown are the values  $\psi(x_1), \psi(x_2), \dots, \psi(x_M)$  (note that we take into account implicitly that  $\psi(0) = \psi(L) = 0$  and the fact that  $\psi$  is odd).

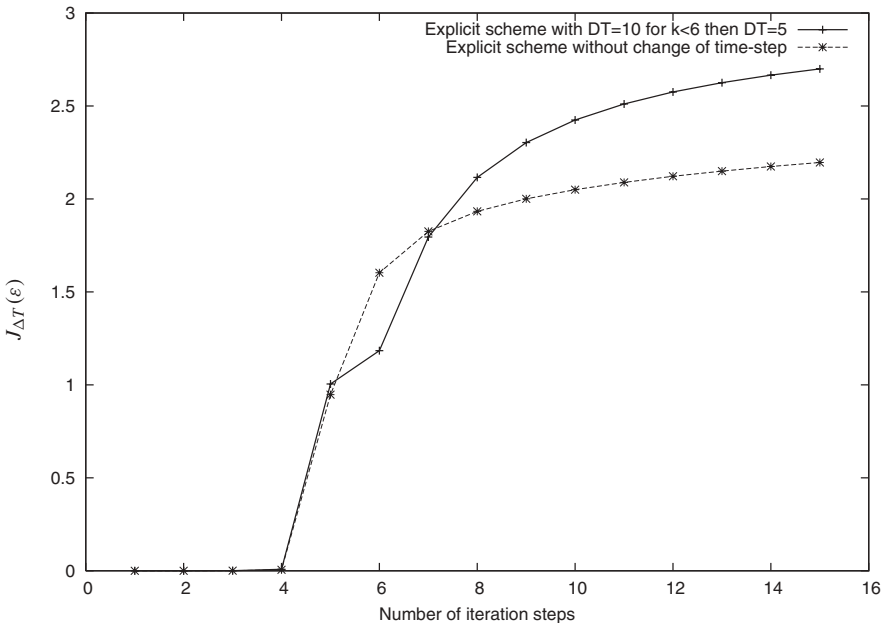


Fig. 4 A change of time step is operated at iteration  $k = 5$

The algorithm is thus as follows, starting from an approximation of  $\psi$  at time  $n\Delta T$   $\psi_j(x_1), \psi_j(x_2), \dots, \psi_j(x_M)$ , we first unfold  $\psi$  by symmetry to get  $\Psi_j = [0, \psi_j(x_1), \dots, \psi_j(x_M), 0, -\psi_j(x_M), \dots, -\psi_j(x_1)]$ . In order to propagate over half a time step through the kinetic operator we change the representation and compute  $\hat{\Psi}_j = \text{fft}(\Psi_j)$ , where  $\text{fft}$  represents the fast Fourier transform algorithm, the evaluation of  $\hat{\Psi}_{j+1/3} = (e^{-\frac{H_0\Delta T}{2i}}) \cdot \hat{\Psi}_j$ , is easy in this Fourier basis since  $(e^{-\frac{H_0\Delta T}{2i}})$  is a diagonal operator. Next we have to propagate over a full time step through the potential operator, and thus, we move back to the physical space and compute first  $\Psi_{j+1/3} = (\text{fft})^{-1}(\hat{\Psi}_{j+1/3})$  then truncate  $\Psi_{j+1/3} : \psi_{j+1/3} = [\Psi_{j+1/3}(2), \dots, \Psi_{j+1/3}(M+1)]$ . The propagation is then obtained by a simple multiplication:

$$\psi_{j+2/3} = [e^{\frac{V(x_1) - \mu(x_1)\varepsilon_j}{i}\Delta T} \psi_{j+1/3}(2), \dots, e^{\frac{V(x_M) - \mu(x_M)\varepsilon_j}{i}\Delta T} \psi_{j+1/3}(M+1)].$$

The last propagation in the Strang split-operator method over half a time step, corresponding to another application of the kinetic operator is done as previously. In order to justify that this approximation maintains the monotonic property exactly, we introduce a discrete scalar product

$$\langle \psi, \varphi \rangle_M = \frac{1}{M+1} \sum_{\ell=1}^M \bar{\psi}(x_\ell) \varphi(x_\ell)$$

that coincides with the standard  $L^2$  inner product for truncated Fourier series of degree  $\leq M$  that are odd.

Still denoting  $\check{\psi} = e^{\frac{H_0\Delta T}{2i}} \psi$ , it is an easy matter to check that this algorithm keeps the property :  $\langle \check{\psi}_1, \psi_2 \rangle_N = \langle \psi_1, \check{\psi}_2 \rangle_N$ , which is the corner stone of the proof of the monotonicity, as e.g. in (12).

The monotonicity is thus guaranteed in the discretized space case as well.

*Remark 3* Full analysis of the convergence of these schemes has yet not been completely understood. Some theoretical results have however been obtained for special choices of  $\alpha$  [19,4].

## References

1. Rabitz, H.: Shaped laser pulses as reagents. *Science* **299**, 525–526 (2003)
2. Rabitz, H., Turinici, G., Brown, E.: Control of quantum dynamics: Concepts, procedures and future prospects. In: Ph. G. Ciarlet, editor, *Computational Chemistry, Special Volume (C. Le Bris Editor) of Handbook of Numerical Analysis, vol X*, 833–887. Elsevier Science B.V. (2003)
3. Shi, S., Woody, A., Rabitz, H.: Optimal Control of Selective Vibrational Excitation in Harmonic Linear Chain Molecules. *J. Chem. Phys.*, **88**, 6870–6883 (1988)
4. Salomon, J.: Limit points of the monotonic schemes for quantum control, *to appear in the Proceedings of the 44th IEEE Conference on decision and Control*, Sevilla, Spain, December 12–15 (2005)
5. Elliott, D.L.: Bilinear systems, University of Maryland. J. Webster (ed.), Wiley Encyclopedia of Electrical and Electronics Engineering Online Copyright © 1999 by John Wiley & Sons
6. Judson, R.S., Rabitz, H.: Teaching lasers to control molecules. *Phys. Rev. Lett.* **68**, 1500–1503 (1992)

7. Levis, R.J., Menkir, G., Rabitz, H.: Selective bond dissociation and rearrangement with optimally tailored, strong field laser pulses. *Science* **292**, 709–713 (2001)
8. Assion, A., Baumert, T., Bergt, M., Brixner, T., Kiefer, B., Seyfried, V., Strehle, M., Gerber, G.: Control of chemical reactions by feedback-optimized phase-shaped femtosecond laser pulses. *Science* **282**, 919–922 (1998)
9. Bergt, M., Brixner, T., Kiefer, B., Strehle, M., Gerber, G.: Controlling the femto-chemistry of  $Fe(CO)_5$ . *J. Phys. Chem. A* **103**, 10381–10387 (1999)
10. Weinacht, T., Ahn, J., Bucksbaum, P.: Controlling the shape of a quantum wavefunction. *Nature* **397**, 233–235 (1999)
11. Bardeen, C.J., Yakovlev, V.V., Wilson, K.R., Carpenter, S.D., Weber, P.M., Warren, W.S.: Feedback quantum control of molecular electronic population transfert. *Chem. Phys. Lett.* **280**, 151–158 (1997)
12. Bardeen, C.J., Yakovlev, V.V., Squier, J.A., Wilson, K.R.: Quantum control of population transfer in green fluorescent protein by using chirped femtosecond pulses. *J. Am. Chem. Soc.* **120**, 13023–13027 (1998)
13. Strang, G.: Accurate partial difference methods I: Linear Cauchy problems. *Arch. Rat. Mech. and An.* **12**, 392–402 (1963)
14. Hornung, T., Motzkus, M., de Vivie-Riedle, R.: Adapting optimal control theory and using learning loops to provide experimentally feasible shaping mask patterns. *J. Chem. Phys.* **115**, 3105–3111 (2001)
15. Tannor, D., Kazakov, V., Orlov, V.: Control of photochemical branching: Novel procedures for finding optimal pulses and global upper bounds. In *Time Dependent Quantum Molecular Dynamics*, edited by Broeckhove J. and Lathouwers L. Plenum, 347–360 (1992)
16. Zhu, W., Rabitz, H.: A rapid monotonically convergent iteration algorithm for quantum optimal control over the expectation value of a positive definite operator. *J. Chem. Phys.* **109**, 385–391 (1998)
17. Maday, Y., Turinici, G.: New formulations of monotonically convergent quantum control algorithms. *J. Chem. Phys.* **118**, 8191–8196 (2003)
18. Bandrauk, A.D., Shen, H.: Exponential split operator methods for coupled Schrödinger equations. *J. Chem. Phys.* **99**, 1185–1193 (1993)
19. Salomon, J.: Phd. thesis. *in progress*
20. Truong, T.N., Tanner, J.J., Bala, P., Andrew McCammon, J., Kouri, D.J., Lesyng, B., Hoffman, D.K.: A comparative study of time dependent quantum mechanical wave packet evolution methods. *J. Chem. Phys.* **96**, 2077–2084 (1992)